J Clust Sci (2012) 23:535–544
DOI 10.1007/s10876-012-0466-y

ORIGINAL PAPER

Excited-State Hydrogen Bonding Dynamics of Hydrogen-Bonded Clusters Formed by of Coumarin Derivatives in Aqueous Solution: A Time-Dependent Density Functional Theory Study

Mingzhen Zhang · Changxin Zhao · Yi Wang

Received: 10 January 2012 / Published online: 7 April 2012
© Springer Science+Business Media, LLC 2012

Abstract The time-dependent density functional theory and the density functional theory are used to investigate the nature of hydrogen bonds formed by the derivative of the coumarin (TFKC) and the water molecules. The ground-state geometry optimizations, electronic excited energies and corresponding oscillation strengths for the TFKC monomer, the hydrogen-bonded TFKC–Water (HBA) dimer, TFKC–Water (HBB) dimer and TFKC–2Water complex are calculated. We find that, upon photoexcitation, the weaker hydrogen bond in the ground state will be affected by the relatively large impact for TFKC in the water. For better understanding the properties of the hydrogen bonds in the excited states, the frontier molecular orbitals of the S0 and S1 states are shown, and we find the obvious electron density transitions form the water molecules to the TFKC monomer. The electron transfer is expected to be the reason the hydrogen bond dynamics happens.

Keywords Excited state · Hydrogen bond dynamics

Introduction

The nature of the hydrogen bond has gained more and more attention because of its importance in physical, chemistry and biology [1–14]. It is central to the understanding of stability and the microscopic structure of the molecule in the solvent [15, 16]. In the 1970s, Ab initio quantum-chemical calculations on hydrogen-bonded complexes were performed for the first time by Janet Del Bene

M. Zhang · C. Zhao (✉) · Y. Wang (✉)
School of Biological Engineering, Dalian Polytechnic University,
Dalian 116034, People's Republic of China
e-mail: zhaochangxin@126.com

Y. Wang
e-mail: dlpu_wangyi@126.com

et al. [17–19], providing a first-principles basis for a description of the hydrogen bond. What's more, the semiempirical methods such as CNDO and INDO were also used widely to study excited-state hydrogen bonding in the past years, providing a wealth of important information about the nature of the hydrogen bond [20–24]. In very recent years, the changes of the hydrogen bonds between the molecules and the solvents upon photoexcitation have been figured out by a variety of theoretical and experimental methods [1, 10–14]. Zhao and Han [25] demonstrated for the first time that the hydrogen bond strengthening can change the excitation energy of the complex and can induce an absorption redshift as well as the hydrogen bond weakening can induce an absorption blueshift. According to this relationship, one can monitor the hydrogen bonding dynamics by the changes of the excited energies of the related states [26–28]. Using this method, Wang investigated the excited-state hydrogen bonding dynamics of hydrogen-bonded complex formed by methyl cyanide and methanol and got the conclusions that the intermolecular hydrogen bonds C≡N···H–O are significantly strengthened in both the low-lying singlet and triplet electronically excited states of the hydrogen-bonded MeCN–MeOH dimer and hydrogen-bonded MeCN–2MeOH complex [26, 27].

In the past decades, coumarin and its derivatives are publicly known as the ideal probes to research the hydrogen bonding dynamics because they are sensitive to the polarity of the solvent and can make kinds of hydrogen bonds in the solvent [1, 10–14]. In very recent years, the derivatives of the coumarin are also found to have a lot of remarkable functions including anticancer activity, antibiotic activity and inhibition of HIV. So the large quantities of the derivatives of the coumarin are synthesized [29–40]. Li et al. [29] synthesize lots of novel coumarin fluorescent dyes and recognize their behavior towards to Cu and Ni. In this paper, we choose one of the derivatives of the coumarin (TFKC, shown in Fig. 1) synthesized by Li to investigate the hydrogen bonding dynamics in the water. Normally, there are two hydrogen acceptor sites in the TFKC molecule, namely, two hydrogen bonds can be formed by the TFKC and water molecules.

To know the detailed aspects of the early-time hydrogen bonding dynamics, we have employed the time-dependent density functional theory (TDDFT) and density functional theory (DFT) methods for the calculations of the optimized geometries, excited energies and vibrational frequencies of the isolated TFKC, hydrogen-bonded TFKC–Water dimer and TFKC–2Water complex in the different states. A decade ago, Jeffrey Reimers calculated the excited-state geometries, frequencies, and vibrationally resolved electronic spectra using TDDFT for the first time. Furthermore, their later works showed the successes and failures of TDDFT for the

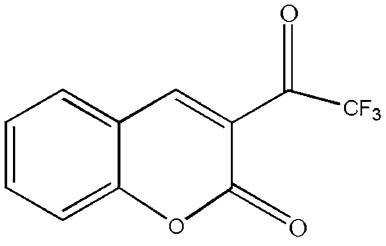

Fig. 1 Chemical construction of the derivative of coumarin (TFKC)

low-lying excited states [24, 41–45]. In recent years, TDDFT and DFT are further proved as the outstanding theoretical tool to investigate the hydrogen bonding dynamics [46–55]. Zhao and co-workers, using the TDDFT and DFT method, first investigated the excited-state hydrogen bond dynamics of coumarin 102 in the phenol. Their theoretical results are in good agreement with the results of the experiments [54]. Sobolewski et al. [46, 47] investigated the equilibrium geometries and vibrational spectra of anthranilic acid and salicylic acid in the S1 excited state using TDDFT, and also demonstrated that TDDTF is a reliable tool to calculate the vibrational absorption spectra in electronically excited states.

Computational Details

DFT was employed to optimize the geometries for the ground-state structures of the isolated TFKC molecule, the isolated water molecule, the hydrogen-bonding TFKC–Water dimers and the TFKC–2Water complex. The energy changes of that in the different electronically excited states were calculated using the TDDFT. Becke's three parameter hybrid exchange functional with Lee–Yang–Parr gradient corrected correlation functional (B3LYP hybrid functional) and 6–31 + (2d.p)G basis set were used in all the calculations. The electronic structure calculations were calculated using the Gaussian 09 program suite.

Results and Discussion

The geometric structures of the isolated TFKC monomer and the hydrogen-bonded TFKC–Water (HBA) dimer, TFKC–Water (HBB) dimer, TFKC–2Water complex in the ground state, which are fully optimized, are shown in Fig. 2. One can clearly see that two hydrogen bonds are formed by the TFKC monomer and the water molecules, which are the same type hydrogen bond(C=O···H–O) in the different hydrogen acceptor sites of the TFKC monomer. To distinguish the two hydrogen bonds, we define the hydrogen bond in Fig. 2b as HBA and the hydrogen bond in Fig. 2c as HBB. Figure 2d shows the structure of the TFKC–2Water complex including both of the two hydrogen bonds. Table 1 lists the calculated bond lengths and angles of the monomer, dimers and complex. By comparing the bond lengths of the TFKC monomer and the hydrogen-bonded dimers, we can see that the lengths of O4–H7 and C8–O1 become slightly longer due to the formation of HBA as well as the lengths of O10–O3 and O5–H9 become similarly longer due to the formation of HBB. One can get the conclusion that the formations of hydrogen bonds between the TFKC and water molecules can slightly change the geometric structure of the TFKC monomer. Furthermore, to inspect the interaction between the two hydrogen bonds, we also calculate the bond lengths and angles of TFKC–2Water complex for comparing. We find that the lengths of O1–H7 (HBA) and O3–H9 (HBB) nearly do not change from dimers to complex as well as the lengths of C9–O1, C10–O3, H7–O4 and H9–O5 do not change either. On the other hand, the angles for O8–O1–H7 and C10–O3–H9 slightly change form 119.2° to 118.1° and 138.3° to 139.1°, respectively, from dimers

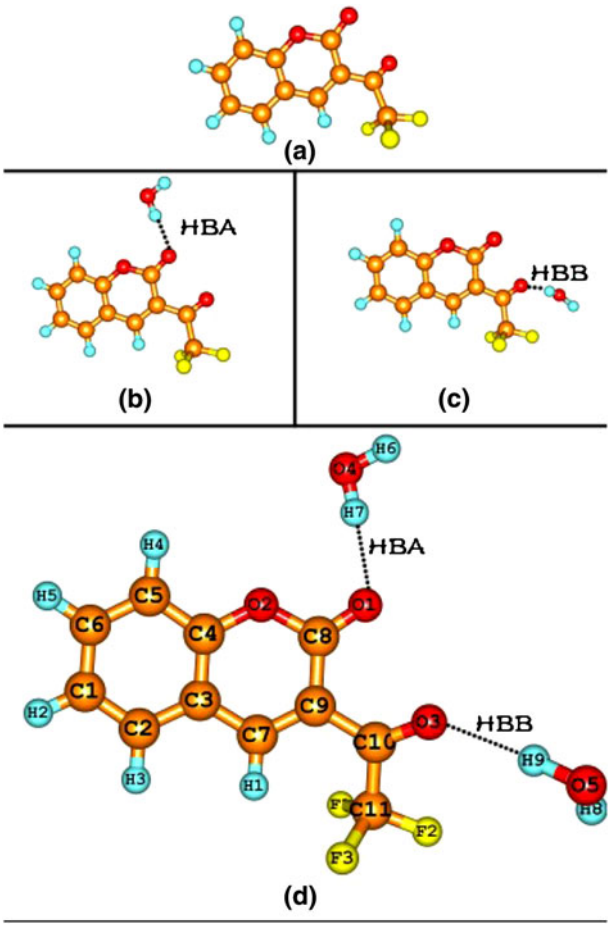

Fig. 2 The geometric structures of the isolate TFKC monomer (**a**) and the hydrogen-bonded TFKC–Water (HBA) dimer (**b**), TFKC–Water (HBB) dimer (**c**), TFKC–2Water complex (**d**) in the ground state

Table 1 Calculated bond lengths L (Å) and bond angles ψ (°) for the isolated TFKC monomer, the isolated water monomer and the hydrogen-bonded TFKC–Water (HBA) dimer, TFKC–Water (HBB) dimer as well as TFKC–2Water complex in ground states

	TFKC	HBA	HBB	TFKC + 2Water	Water
L O1–H7		2.00467		2.01794	
L O3–H9			2.09510	2.09686	
L C8–O1	1.95920	1.20279		1.20253	
L C10–O3	1.20316		1.20632	1.2062	
L H7–O4		0.97106		0.97066	0.96344
L H9–O5			0.96794	0.96775	0.96344
ψ C8–O1–H7		119.2		118.1	
ψ C10–O3–H9			138.3	139.1	

to complex. It implies that the interaction between the two hydrogen bonds exists. But this influence is very weak and even can be neglected because of the extreme little changes of the geometric structures. Accordingly we believe that the nature of the two hydrogen bonds do not change from the dimers to complex.

Interestingly, by comparing the bond length of HBA and HBB for both dimer and complex in the ground state, we can see that the bond length of HBA is shorter than that of HBB which corresponds to that HBA is stronger than HBB. The total atomic charges of the TFKC–Water (HBA), TFKC–Water (HBB) and TFKC–2Water complex in the ground state are shown in Table 2. We can see that, for the TFKC–Water (HBA) dimer, the atomic charges of the O1 and H7 are −0.277 and 0.391 while that of O3 and H9 for the TFKC–Water (HBB) are −0.218 and 0.384. Furthermore, for the TFKC–2Water complex, the atom charges of O1, H7, O3 and H9 are −0.28, 0.388, −0.218 and 0.384, respectively. As we all know, the higher negative charge of the oxygen atom, as well as the higher positive charge of the hydrogen atom, can significantly facilitate the forming of the hydrogen bond. So the atomic charges provide the further evidence that the HAB is stronger than HBB for the dimers and complex in the ground state.

Table 3 lists the electronic transition energies and corresponding oscillation strengths of the TFKC monomer, the hydrogen-bonded TFKC–Water (HBA) dimer, TFKC–Water (HBB) dimer and TFKC–2Water complex. For comparing intuitively, we integrate the data of electronic transition energies and corresponding oscillation strengths and draw the absorption spectrums shown in Fig. 3. From the Fig. 3, we can see that there are mainly three absorption peak areas which are labeled by (a), (b) and (c). The three absorption peak areas correspond to different excited states. We interestingly see that the hydrogen bonding dynamics in different states shows absolutely different properties. Firstly, we focus our attention to the area (a). One can clearly see that the redshifts are found in order of TFKC monomer, TFKC–Water (HBA) dimer, TFKC–Water (HBB) dimer, TFKC–2Water complex. According to Zhao's conclusion mentioned above, we can know that, upon photoexcitation, HBA and HBB are strengthened simultaneously in the corresponding states of this area for the dimers. At the same time, by the joint factors of the two hydrogen bonds, the doubly hydrogen-bonded TFKC–2Water complex has a certain extent redshift. Furthermore, we also see that, by comparing the two dimers, the redshift of TFKC–Water (HBB) dimer is much more than that of TFKC–Water (HBA) dimer. As we all know that HBA and HBB are the same type hydrogen bonds. Hence, we can get the conclusion the extent of the redshift corresponds to the extent of the strengthening of the hydrogen bond. So the strengthening of HBB is much more than that of HBA, namely, HBB is affected more than HBA upon photoexcitation in the corresponding

Table 2 The total atomic charges of the TFKC–Water (HBA), TFKC–Water (HBB) and TFKC–2Water complex in the ground state

	HBA	HBB	TFKC–2Water
O1	−0.277		−0.280
O3		−0.218	−0.218
H7	0.391		0.388
H9		0.384	0.384

Table 3 Calculated electronic transition energies (in eV) and corresponding oscillation strengths (in the parentheses) of the low-lying electronically excited states for the isolated TFKC monomer, isolated water monomer, the hydrogen-bonded TFKC–Water (HBA) dimer, TFKC–Water (HBB) dimer and TFKC–2Water complex

	TFKC	HBA	HBB	TFKC–2Water	Water
S1	3.304 (0.003)	3.307 (0.096)	3.338 (0.018)	3.378 (0.018)	7.959 (0.074)
S2	3.533 (0.111)	3.541 (0.096)	3.465 (0.092)	3.478 (0.075)	10.128 (0.000)
S3	4.128 (0.307)	3.812 (0.002)	3.828 (0.003)	3.688 (0.001)	10.159 (0.116)
S4	4.217 (0.016)	4.104 (0.342)	4.065 (0.346)	3.771 (0.003)	11.451 (0.016)
S5	4.871 (0.001)	4.348 (0.002)	4.213 (0.005)	4.043 (0.366)	12.019 (0.002)
S6	5.186 (0.063)	4.884 (0.001)	4.887 (0.003)	4.338 (0.002)	12.375 (0.014)
S7	5.448 (0.014)	5.200 (0.075)	5.124 (0.056)	4.931 (0.002)	12.565 (0.000)
S8	5.513 (0.008)	5.365 (0.002)	5.441 (0.002)	5.110 (0.065)	13.491 (0.004)
S9	5.588 (0.099)	5.474 (0.017)	5.458 (0.037)	5.225 (0.004)	13.883 (0.133)
S10	5.681 (0.017)	5.533 (0.096)	5.495 (0.045)	5.343 (0.004)	14.019 (0.120)
S11	5.895 (0.008)	5.623 (0.023)	5.604 (0.029)	5.421 (0.077)	14.114 (0.038)
S12	5.926 (0.005)	5.694 (0.011)	5.620 (0.002)	5.507 (0.019)	15.252 (0.232)
T1	2.531 (0.000)	2.556 (0.000)	2.501 (0.000)	2.529 (0.000)	7.283 (0.000)
T2	2.898 (0.000)	2.887 (0.000)	2.975 (0.000)	2.986 (0.000)	9.349 (0.000)
T3	3.112 (0.000)	3.072 (0.000)	3.048 (0.000)	3.021 (0.000)	9.699 (0.000)
T4	3.906 (0.000)	3.808 (0.000)	3.822 (0.000)	3.684 (0.000)	10.782 (0.000)
T5	4.004 (0.000)	4.007 (0.000)	3.908 (0.000)	3.764 (0.000)	11.195 (0.000)
T6	4.299 (0.000)	4.056 (0.000)	4.006 (0.000)	4.006 (0.000)	11.578 (0.000)

states of this area. Then we pay attention to the area (b) in Fig. 3. One can see that in this area, the hydrogen bond dynamics is extremely similar to area (a). So one can get the same conclusions in this area. The more interesting thing happens in the area (c), one can see that, by comparing to the TFKC monomer, the redshift is found for the TFKC–Water (HBB) dimer while the blueshift is found for the TFKC–Water (HBA) dimer. This obviously shows that the HBB is strengthened while HBA is weakened in the corresponding states of this area. And we also see that for the TFKC–2Water complex the redshift is found by comparing to the TFKC monomer. So one can deduced, in the corresponding states of the area (c), the extent of the strengthening for HBB must be greater than that of the weakening for HBA. To sum up the above conclusions, HBB is demonstrated to be affected more than HBA upon photoexcitation, namely, the weaker hydrogen bond in the ground state will be affected by the relatively large impact upon photoexcitation.

The frontier molecular orbitals (MOs) of the TFKC–Water (HBA) dimer,TFKC–Water (HBB) dimer and TFKC–2Water complex are shown in Fig. 4 as well as the dominant contributions of the orbital transitions are shown in Table 4. We mainly pay attention to S0-S1 state, so only a few of frontier MOs are shown in Fig. 4. From Fig. 4, one can note that the electron density of HOMO is localized in both the TFKC monomer and the oxygen atoms of water molecules in all the dimers and complex. However, the electron density of LUMO is delocalized to the TFKC

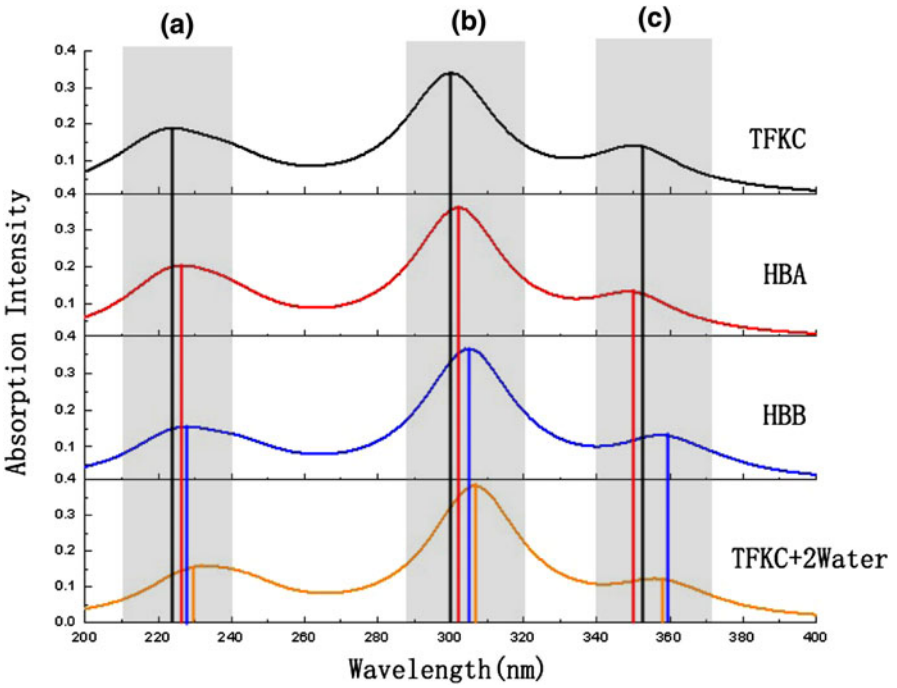

Fig. 3 The absorption spectrums of the TFKC monomer, TFKC–Water (HBA) dimer, TFKC–Water (HBB) dimer and TFKC–2Water complex

monomer. Thus, it is obvious that the electron density of the oxygen atom of the water molecule must be lowered, namely, the corresponding negative charges must be lowered. This logically induces the decrease of the positive charge for the hydrogen atom of the water molecule. Hence, in the S1 state, the hydrogen bond is weakened. This conclusion is in good agreement with the result of the electronic transition energies. So it is expected that the electron transfer is the reason the hydrogen bonding dynamics happens.

Conclusion

In this work, we theoretically investigate the nature of hydrogen bonds between the TFKC monomer and the water molecule. We see that there are two same type hydrogen bond (C≡N···H–O) formed by the TFKC monomer and water molecules. By studying the bond lengths, bond angles and atom charges, we get the conclusion that HAB is much stronger than HBB for the dimers and complex in the ground state. Furthermore, we also calculate the electronic energies and draw the absorption spectrum, we gain the information that in the excited states HBB is affected more than HBA upon photoexcitation in the corresponding states of the three absorption peak areas. To know the reason the hydrogen bonding dynamics happens, the frontier MOs of the TFKC–Water (HBA) dimer, TFKC–Water (HBB) dimer and

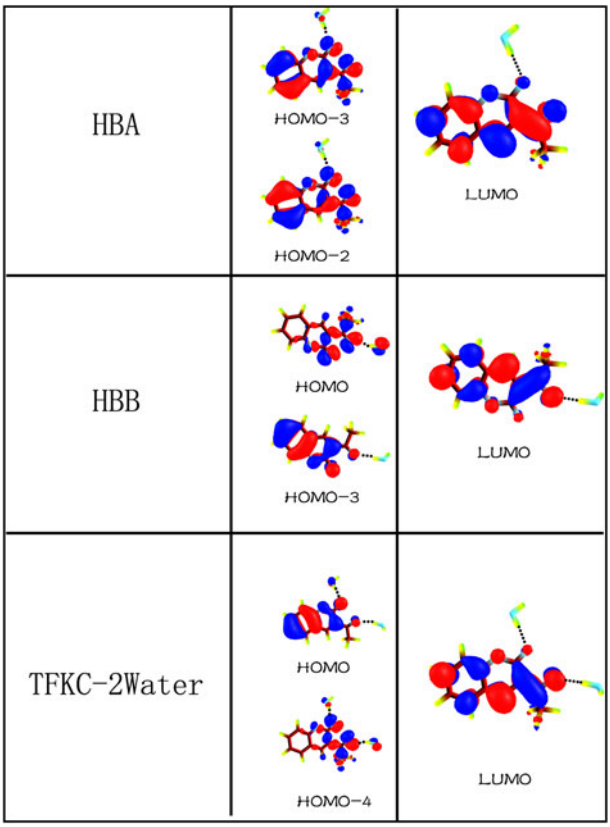

Fig. 4 The frontier MOs of the TFKC–Water (HBA), TFKC–Water (HBB) and TFKC–2Water complex

Table 4 Dominant contributions of the orbital transitions for TFKC–Water (HBA) dimer, TFKC–Water (HBB) dimer and TFKC–2Water complex from S0 state to S1 state

	S0–S1
HBA	HOMO-3 → LUMO (45.54 %)
	HOMO-2 → LUMO (49.87 %)
HBB	HOMO → LUMO (32.10 %)
	HOMO-3 → LUMO (56.54 %)
TFKC–2Water	HOMO → LUMO (32.46 %)
	HOMO-4 → LUMO (57.59 %)

TFKC–2Water complex are also shown. From the frontier MOs, a distinct electron transfer from water molecule to the TFKC monomer is found and is expected as the main reason the hydrogen bonding dynamics happens in S1 state.

To sum up the above conclusions, it shows the interesting regulation that the weaker hydrogen bond in the ground state will be affected by the relatively large impact upon photoexcitation for the TFKC in the water.

References

1. K. L. Han and G. J. Zhao *Hydrogen Bonding and Transfer in the Excited State* (Wiley, Chichester, 2010).
2. M. Simona and J. James (2010). *J. Phys. Chem. A.* **114**(51), 13376–13380.
3. D. Vaibhav, R. Prakash, and B. Prasad (2010). *J. Mol. Struct. Theochem.* **962**, 97–100.
4. N. Y. Indra, M. A. Subha, and G. Sastry (2010). *J. Phys. Chem. B.* **114**, (51), 17162–17171.
5. K. Makoto, N. Kennichi, and L. Yunfeng (2010). *J. Am. Chem. Soc.* **132**, (51), 18281–18286.
6. P. Seokan and K. Hae-Jo (2010). *Chem. Commun.* **46**, 9197–9199.
7. M. Meot-Ner (2005). *Chem. Rev.* **105**, 213–284.
8. T. Steiner (2002). *Angew. Chem. Int. Ed.* **41**, 48–76.
9. C. J. Fecko, J. D. Eaves, J. J. Loparo, A. Tokmakoff, and P. L. Geissler (2003). *Science* **301**, 1698–1702.
10. G. J. Zhao and K. L. Han (2008). *Biophys. J.* **94**, 38.
11. K. L. Han and G. Z. He (2008). *J. Photochem. Photobiol. C.* **8**, 55.
12. G. J. Zhao and K. L. Han (2009). *J. Phys. Chem. A.* **113**, 14329.
13. G. J. Zhao and K. L. Han (2009). *J. Phys. Chem. A.* **113**, 4788.
14. E. Krystkowiak and A. Maciejewski (2011). *Phys. Chem. Chem. Phys.* **13**, 11317–11324.
15. G. J. Zhao, R. K. Chen, M. Sun, G. Y. Li, J. Liu, Y. Gao, K. L. Han, X. Yang, and L. C. Sun (2008). *Chem. Eur. J.* **14**, 6935–6947.
16. Y. Nagasawa, A. P. Yartsev, K. Tominaga, A. E. Johnson, and K. Yoshihara (1994). *J. Chem. Phys.* **101**, 5717.
17. D. B. Janet and J. A. Pople (1969). *Chem. Phys. Lett.* **47**, 426–428.
18. D. B. Janet and J. A. Pople (1970). *J. Chem. Phys.* **52**, 4858.
19. D. B. Janet and M. T. Jordan (2001). *J. Mol. Struct. Theochem.* **573**, 11–23.
20. S. N. Datta, B. S. Prabhakar, and V. Nehra (1999). *J. Phys. Chem. B.* **103**, 2291–2296.
21. J. Rezac and P. Hobza (2012). *J. Chem. Theory Comput.* **8**, 141–151.
22. M. I. Bernal, M. C. Martins, C. Millot, and M. F. Ruiz (2000). *J. Comput. Chem.* **21**, (7), 572–581.
23. Y. L. Wang and J. R. Gunn (1999). *Int. J. Quantum Chem.* **73**, 357–367.
24. J. Zeng, N. S. Hush, and J. R. Reimers (1993). *J. Chem. Phys.* **99**, 1508.
25. G. J. Zhao and K. L. Han (2008). *ChemPhysChem.* **9**, 1842–1846.
26. H. F. Wang, M. S. Wang, E. F. Liu, M. L. Xin, and C. L. Yang (2011). *Comput. Theor. Chem.* **964**, 243–247.
27. H. F. Wang, M. S. Wang, M. L. Xin, E. F. Liu, and C. L. Yang (2011). *Cent. Eur. J. Phys.* **9**, 792–799.
28. J. J. Tan, C. Hao, N. N. Wei, M. X. Zhang, and X. Y. Dai (2011). *J. Theor. Comput. Chem.* **10**, (3), 1–8.
29. H. Q. Li, C. Li, and J. X. Li (2011). *Dyes Pigments* **91**, (3), 309–316.
30. S. Koneni, K. Abdhesh, and K. Manoj (2010). *Bioorg. Med. Chem. Lett.* **20**, (24), 7205–7211.
31. G. J. Zhao, B. H. Northrop, P. J. Stang, and K. L. Han (2010). *J. Phys. Chem. A.* **114**, 3418.
32. B. M. Antoaneta, S. Nagahiro, and T. Osamu (2010). *Appl. Surf. Sci.* **257**, (5), 1792–1799.
33. S. Abhigyan and H. Partha (2010). *Chem. Phys. Lett.* **501**, (1–3), 33–38.
34. J. Farnaz, J. Nafiseh, and O. M. Amiri (2010). *Tetrahedron* **66**, (49), 9508–9511.
35. A. I. Mosa, A. A. Adel, and J. M. Yousef (2011). *Spectrochim. Acta A.* **81**, (1), 35–43.
36. D. Tehsina, R. Claire, and W. Christina (2011). *Bioorg. Med. Chem. Lett.* **21**, (19), 5770–5773.
37. M. Yanez, J. Leiro, and J. A. Arranz (2011). *Basic Clin. Pharmacol. Toxicol.* **109**, (2), 47–48.
38. P. Mehtab, A. Akhtar, and M. A. Mohammed (2011). *Chem. Pap.* **65**, (5), 735–738.
39. J. Amit, S. Vijay, and R. Rajkumar (2011). *Dyes Pigments* **91**, (1), 33–43.
40. P. K. Teskac, P. Stane, and G. Biljana (2011). *Int. J. Pharm.* **416**, (1), 384–393.
41. Z. L. Cai and J. R. Reimers (2000). *J. Chem. Phys.* **112**, 527.
42. Z. L. Cai, D. J. Tozer, and J. R. Reimers (2000). *J. Chem. Phys.* **113**, 7084.
43. Z. L. Cai and J. R. Reimers (2002). *J. Phys. Chem. A.* **106**, 8769.
44. Z. L. Cai and J. R. Reimers (2005). *J. Phys. Chem. A.* **109**, 1576.
45. M. G. Dahlbom and J. R. Reimers (2004). *Mol. Phys.* **103**, 1057.
46. A. L. Sobolewski and W. Domcke (2004). *J. Phys. Chem. A.* **108**, 10917.
47. A. L. Sobolewski, W. Domcke, and C. Hattig (2006). *J. Phys. Chem. A.* **110**, 6301.
48. G. J. Zhao, J. Y. Liu, L. C. Zhou, and K. L. Han (2007). *J. Phys. Chem. B.* **111**, 8940.

49. G. J. Zhao and K. L. Han (2008). *J. Comput. Chem.* **29**, 2010.
50. G. J. Zhao, K. L. Han, and P. J. Stang (2009). *J. Chem. Theory Comput.* **5**, 1955–1958.
51. G. J. Zhao and K. L. Han (2007). *J. Chem. Phys.* **127**, 024306.
52. G. J. Zhao, B. H. Northrop, K. L. Han, and P. J. Stang (2010). *J. Phys. Chem. A.* **114**, 9007–9013.
53. G. J. Zhao and K. L. Han (2007). *J. Phys. Chem. A.* **111**, 9218–9223.
54. G. J. Zhao and K. L. Han (2007). *Phys. Chem. A.* **111**, 2469–2474.
55. G. J. Zhao and K. L. Han (2012). *Acc. Chem. Res.* **45**, 404–413.